# Shmt1 Heterozygosity Impairs Folate-Dependent Thymidylate Synthesis Capacity and Modifies Risk of Apc$^{min}$-Mediated Intestinal Cancer Risk

Amanda J. MacFarlane[1], Cheryll A. Perry[1], Michael F. McEntee[2], David M. Lin[3], and Patrick J. Stover[1]

## Abstract

Folate-mediated one-carbon metabolism is required for the *de novo* synthesis of purines, thymidylate, and *S*-adenosylmethionine, the primary cellular methyl donor. Impairments in folate metabolism diminish cellular methylation potential and genome stability, which are risk factors for colorectal cancer (CRC). Cytoplasmic serine hydroxymethyltransferase (SHMT1) regulates the partitioning of folate-activated one-carbons between thymidylate and *S*-adenosylmethionine biosynthesis. Therefore, changes in SHMT1 expression enable the determination of the specific contributions made by thymidylate and *S*-adenosylmethionine biosynthesis to CRC risk. *Shmt1* hemizygosity was associated with a decreased capacity for thymidylate synthesis due to downregulation of enzymes in its biosynthetic pathway, namely thymidylate synthase and cytoplasmic thymidine kinase. Significant *Shmt1*-dependent changes to methylation capacity, gene expression, and purine synthesis were not observed. *Shmt1* hemizygosity was associated with increased risk for intestinal cancer in *Apc$^{min/+}$* mice through a gene-by-diet interaction, indicating that the capacity for thymidylate synthesis modifies susceptibility to intestinal cancer in *Apc$^{min/+}$* mice. *Cancer Res; 71(6); 2098–107. ©2011 AACR.*

## Introduction

The interactions among nutrients and genetic factors play an important role in the development of numerous cancers including colorectal cancer (CRC). A strong, inverse association of folate status and CRC has been demonstrated; individuals with lowest dietary folate intake show a 40% to 60% increase in CRC risk when compared with individuals with highest folate intake (1–3). Genetic variation that alters folate metabolism and utilization also influences cancer risk (2). The mechanism by which folate metabolism alters CRC risk is not known, which has led to concerns regarding the potential impact of elevated dietary folate intake and folate fortification initiatives on CRC incidence (4, 5).

Folate-mediated one-carbon (1C) metabolism is a metabolic network of interdependent biosynthetic pathways required for the *de novo* biosynthesis of purines, dTMP, and the remethylation of homocysteine to methionine (Fig. 1; ref. 6). Methionine can be converted to *S*-adenosylmethionine (AdoMet), the major 1C donor for cellular methylation reactions including the methylation of DNA, RNA, phospholipids, proteins, and small molecules (6, 7). Impairments in 1C metabolism due to nutrient deficiencies and/or single-nucleotide polymorphisms diminish dTMP synthesis, leading to elevated dUTP pools, increased rates of dUTP misincorporation into DNA, and consequently futile cycles of DNA excision repair and chromosomal strand breaks (8–10). Altered folate metabolism also influences chromatin methylation patterns, including genome-wide CpG hypomethylation and site-specific hypermethylation and altered histone methylation, which modify gene expression patterns (11–13). Therefore, the loss of DNA integrity due to increased genome instability and/or changes in gene expression due to altered genome methylation are candidate causal pathways for folate-mediated CRC.

Cytoplasmic serine hydroxymethyltransferase (SHMT1) acts as a metabolic switch that regulates the partitioning of 1C units between the dTMP and methionine biosynthetic pathways (Fig. 1; ref. 14). Folate-activated 1Cs can be derived in the cytoplasm from formate through the *Mthfd1* gene product or from serine through SHMT1 to support methionine and thymidylate biosynthesis (Fig. 1). Thymidylate synthesis can occur in both the cytoplasm and nucleus (7, 15). When expressed, SHMT1 preferentially partitions methylenetetrahydrofolate (methyleneTHF) into the dTMP synthesis pathway through the small ubiquitin-like modifier (SUMO)-mediated compartmentalization of the dTMP biosynthetic pathway components in the nucleus during S phase (14, 16). In the

**Authors' Affiliations:** [1]Division of Nutritional Sciences and [3]Department of Biomedical Sciences, Cornell University, Ithaca, New York; [2]Department of Pathobiology, College of Veterinary Medicine, University of Tennessee, Knoxville, Tennessee

Current address for A.J. MacFarlane: Nutrition Research Division, Food Directorate, Health Products and Food Branch, Health Canada, Ottawa, Ontario, Canada K1A 0K9.

**Corresponding Author:** Patrick J. Stover, Division of Nutritional Sciences, Cornell University, 127 Savage Hall, Ithaca NY 14850. Phone: 607 255 8001; Fax: 607 255 2698; E-mail: pjs13@cornell.edu

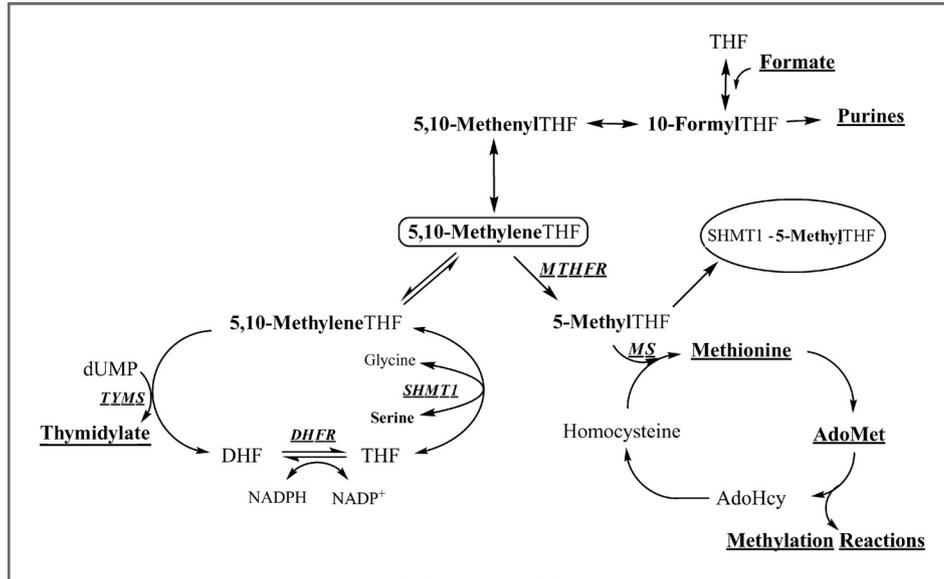*American Association for Cancer Research*

**Figure 1.** Folate-mediated 1C metabolism. THF-mediated 1C metabolism is required for the synthesis of purines and thymidylate and the remethylation of homocysteine to methionine. The hydroxymethyl group of serine is the major source of 1C units which are generated in the mitochondria in the form of formate, or in the cytoplasm through the activity of SHMT1. Mitochondrial-derived formate can enter the cytoplasm and function as a 1C unit for folate metabolism. 5,10-MethyleneTHF can be generated in the cytoplasm from formate or serine and the sources of 5,10-methyleneTHF exist in equilibrium. The SHMT1 enzyme also inhibits homocysteine remethylation by sequestering 5-methylTHF in the cytoplasm. The *de novo* thymidylate synthesis pathway involves the 3 enzymes SHMT1, TYMS, and DHFR, whereas the salvage pathway involves TK1. The 1C unit is labeled in bold. DHFR, dihydrofolate reductase.

cytoplasm, SHMT1 tightly binds and sequesters 5-methylTHF making it unavailable for the methionine cycle, inhibiting AdoMet synthesis, and reducing the cellular methylation potential (14).

Aberrant Wnt signaling resulting from altered *Apc* gene expression is observed in approximately 85% of cases of sporadic CRC (reviewed in ref. 17). In rats, folate deficiency has previously been associated with strand breaks in the mutation cluster region within the *Apc* gene, which were inversely correlated with *Apc* gene expression (18). Folate-mediated strand breaks in the *Apc* gene could be due to hypomethylation of the gene or genomic instability induced by misincorporation of uracil into genomic DNA. In the present study, we have modified the expression of SHMT1 in mice to determine the role(s) played by *de novo* purine, thymidylate, and methionine synthesis in the development of *Apc^min*-mediated intestinal cancer.

## Materials and Methods

### Mice

SHMT1 null (*Shmt1^{-/+}*) mice were generated as previously described (19) and backcrossed a minimum of 10 generations onto the C57BL/6J strain. Mice were genotyped using the forward primer 5′-GACACTGTTCACATCCCTC-3′ and the reverse primer 5′-CAAAACATTCGGGAGCCTC-3′. The forward primer corresponds to an intron 6 sequence located 5′ to a *loxP* site and exon 7 and the reverse primer corresponds to an intron 7 sequence located downstream of a 3′ *loxP* site (19). C57BL/6J-*Apc^Min*/J (*Apc^{min/+}*) mice were obtained from The Jackson Laboratory. Genotyping of *Apc^{min/+}* mice was

performed using the following primers recommended by The Jackson Laboratory protocol: wild-type forward primer 5′-GCCATCCCTTCACGTTAG-3′, Min forward primer 5′-TTCTGAGAAAGACAGAAGTTA-3′, and a common reverse primer 5′-TTCCACTTTGGCATAAGGC-3′. *Shmt1^{-/+}* mice were mated to *Apc^{min/+}* mice. Double heterozygous offspring were intercrossed to achieve *Apc^{min/+}Shmt1^{+/+}*, *Apc^{min/+}Shmt1^{-/+}* or *Apc^{min/+}Shmt1^{-/-}* mice.

Mice were maintained under specific pathogen-free conditions at the Cornell University Transgenic Mouse Core Facility in accordance with standard use protocols and animal welfare regulations. All study protocols were approved by the Institutional Animal Care and Use Committee of Cornell University and conform to the NIH Guide for the Care and Use of Laboratory Animals.

### Diets

Mice were randomly weaned onto either a control (AIN-93G; Dyets, Inc.) diet or a modified AIN-93G diet lacking folic acid and choline (Dyets, Inc.) at 3 weeks of age. The control diet contained 2 mg/kg folic acid and 2.5 g/kg choline bitartrate, and the folate/choline-deficient (FCD) diet contained 0 mg/kg folic acid and 0 g/kg choline bitartrate. Mice were maintained on the diet for 5 weeks (*Apc^{+/+}*) or 11 weeks (*Apc^{min/+}*).

### Immunohistochemistry

The colons from wild-type FVB/NJ (Friend virus B NIH Jackson) mice were fixed as Swiss rolls in 10% neutral-buffered formalin. Samples were embedded in paraffin and sectioned (5 μm). Polyclonal sheep anti-SHMT1 antibody was used to

probe the sections for cellular localization of SHMT1 (20). Nonimmune sheep serum was used as a negative control. Biotinylated rabbit anti-sheep IgG was used as the secondary antibody. SHMT1 was visualized with AEC (3-amino-9-ethylcarbazole) developer (Dako). Sections were counterstained using Gill's hematoxylin 2 (Sigma). Coverslips were mounted using Fluoromount-G (Sigma).

### Tumor assessment

The small intestine and colon were removed, flushed with cold PBS, opened longitudinally, and laid flat lumen side up for examination using a dissecting microscope as previously described (21). Tumors were counted according to intestinal location (small intestine or colon) and their diameter measured by a pathologist-trained investigator who was blinded to the genotype of the intestinal specimen. Tumor load is a function of tumor number and area and was calculated as the total tumor area per mouse.

### Plasma and tissue folate determination

Folate concentration of plasma and tissues was quantified using the *Lactobacillus casei* microbiological assay (14). Protein concentration was quantified (22).

### Detection of uracil in nuclear DNA

Uracil content in hepatic nuclear DNA was determined by gas chromatography/mass spectrometry as previously described (19). Uracil content in liver nuclear DNA has been shown to correlate with uracil content in colonic nuclear DNA in $Shmt1^{-/+}$ mice (A.J. MacFarlane and P.J. Stover, in preparation).

### Tissue AdoMet and AdoHcy determination

The animal feeding cycle was synchronized prior to tissue harvest to ensure AdoMet levels reflected homocysteine remethylation capacity with minimal contributions from dietary methionine. Food was removed 24 hours before killing the animals. After 12 hours, each animal was given one food pellet and the animals were killed 12 hours later by cervical dislocation. Tissues were harvested and immediately flash frozen and stored at $-80°C$ until analysis. Frozen tissues were sonicated in 500 μL of 0.1 mol/L NaAcO buffer (pH 6), and protein was precipitated by adding 312 μL of 10% perchloric acid to each sample. After vortexing, samples were centrifuged at $2,000 \times g$ for 10 minutes at $4°C$. AdoMet and AdoHcy (*S*-adenosylhomocysteine) were determined by high-performance liquid chromatography as described previously (14). AdoMet and AdoHcy values were normalized to cellular protein content (22).

### Western blot analysis

Total protein was extracted and quantified from frozen tissue (22). Immunoblotting was performed as previously described (19). The membranes were visualized using the SuperSignal West Pico chemiluminescent substrate system (Pierce). For actin detection, polyclonal rabbit antiactin antibody conjugated to horseradish peroxidase (HRP; Abcam) was diluted 1:40,000. For SHMT1 detection, sheep anti-mouse SHMT1 antibody (20) was diluted 1:10,000, and rabbit anti-sheep IgG secondary anti-

body conjugated to HRP (Pierce) was diluted 1:20,000. For thymidylate synthase (TYMS) detection, monoclonal mouse anti-TYMS antibody (Invitrogen) was diluted 1:3,000 and goat anti-mouse IgG secondary antibody conjugated to HRP (Pierce) was diluted 1:5,000. For cytoplasmic thymidine kinase (TK1) detection, monoclonal mouse anti-TK1 antibody (Abcam) was diluted 1:1,000, and horse anti-mouse IgG secondary antibody conjugated to HRP (Cell Signaling Technology) was diluted 1:1,000. Densitometric analysis of Western blots was performed using Scion Image for Windows (Scion Corporation). Three animals per group were included in the analysis. Values were normalized to glyceraldehyde 3 phosphate dehydrogenase. Densitometric data are presented relative to the mean of wild-type animals fed the control diet.

### Mouse embryonic fibroblast isolation and maintenance

Mouse embryonic fibroblasts (MEF) were freshly isolated as described in the work of MacFarlane and colleagues (19). Cells were cultured in α-minimal essential medium (Hyclone Laboratories) supplemented with 10% fetal calf serum (FCS; Hyclone Laboratories), 0.1 mmol/L nonessential amino acids (Invitrogen), 1 mmol/L sodium pyruvate (Invitrogen), and penicillin/streptomycin (Invitrogen) and incubated at $37°C$ in a 5% $CO_2$ atmosphere.

### Purine synthesis assay

[$^{14}$C]Formate and [$^3$H]hypoxanthine are precursors for purine nucleotide biosynthesis through the *de novo* and salvage pathways, respectively (23). For tracer experiments, FCS was dialyzed against PBS for over 24 hours with 6 buffer changes to remove folate and other small molecules and then charcoal treated to remove any residual folate. The tracer medium was Defined Minimal Essential Medium (Hyclone Laboratories) that lacked glycine, serine, methionine, hypoxanthine, and folate but was supplemented with 10% dialyzed and charcoal-treated FCS, 1 mg/L pyridoxyl-L-phosphate, 200 μmol/L methionine, 20 nmol/L leucovorin, 2 nmol/L [$^3$H]hypoxanthine (Moravek), and 20 μmol/L [$^{14}$C]formate (Moravek). MEFs were plated $2 \times 10^4$ cells/well in 6-well plates and grown at $37°C$, 5% $CO_2$ in tracer medium until confluent and harvested. The cell pellets were stored at $-80°C$. Nuclear DNA was isolated using a DNA blood kit from Qiagen, RNase A treated and isotope levels quantified on a Beckman LS6500 scintillation counter in dual disintegrations per minute (dpm) mode.

### Thymidylate synthesis assay

[$^{14}$C]Deoxyuridine and [$^3$H]thymidine are precursors for thymidylate nucleotide biosynthesis through the *de novo* and salvage pathways, respectively. The tracer medium was Defined Minimal Essential Medium (Hyclone Laboratories) that lacked glycine, serine, methionine, hypoxanthine, and folate but was supplemented with 10% dialyzed and charcoal-treated FCS, 1 mg/L pyridoxyl-L-phosphate, 200 μmol/L methionine, 20 nmol/L leucovorin, 500 nmol/L [$^3$H]thymidine (Moravek), and 10 μmol/L [$^{14}$C]deoxyuridine (Moravek). MEFs were plated $2 \times 10^4$ cells/well in 6-well plates and grown at $37°C$, 5% $CO_2$ in tracer medium until confluent and harvested. The cell pellets were stored at $-80°C$. Nuclear DNA was

isolated using a DNA blood kit from Qiagen with RNase A treatment and isotope levels quantified on a Beckman LS6500 scintillation counter in dual dpm mode. Data were normalized to the wild-type MEF line in each independent experiment.

## Microarray analysis

Microarray analysis was performed on colon tissue from *Shmt1*$^{+/+}$, *Shmt1*$^{-/+}$, and *Shmt1*$^{-/-}$ mice fed the AIN-93G minus folate and choline diet. Total RNA was isolated from colons and 50 ng was amplified using the Nugen Ovation V2 kit (Nugen). Amplified RNA from 9 mice (3 independently processed samples from each genotype) was hybridized to Affymetrix 430A mouse gene expression chips (Affymetrix) and scanned using an Affymetrix GeneChip 3000 scanner. The raw array data were processed using GCOS software to obtain signal values scaled to a default target of 500. Further statistical data analysis was performed using R (24). The signal values were log$_2$-transformed after offset by 8, and gene filtering was applied to include only the 19,871 probe sets having at least one present call in the data set. A 2-sample *t* test was applied on the normalized log ratio of each probe set. At a *P* value cutoff point of 0.01, 134 differential genes between wild-type and null mice were selected whereas 229 differential genes were selected between wild-type and heterozygous mice (Supplementary Table S1). Because only 3 replicates were performed for each sample, multiple testing correction was not performed. The microarray data have been deposited in the National Center for Biotechnology Information's Gene Expression Omnibus (GEO; ref. 25) and are accessible through GEO Series accession number GSE14645.

## Quantitative RT-PCR

Gene expression levels of candidate genes identified in the microarray screen were tested by quantitative reverse transcription PCR (qRT-PCR) using the Taqman-based Universal Probe Library (Roche). Colon RNA used in the microarray screen was primed with oligo(dT) and reverse transcribed with Superscript III (Invitrogen) to generate cDNA template. Quantitative RT-PCR primers were designed using the Universal Probe Library Assay Design Center, (Roche; ref. 26) and validated on an Applied Biosystems 7500 machine by comparison against a standard curve generated with rodent GAPDH control primers (Applied Biosystems). Relative quantitation analysis was then performed in triplicate for all 9 samples. Genes tested, Affymetrix ID, primer sequences, and universal probe library numbers used are in Supplementary Table S2.

## Statistical analyses

Differences between 2 groups were determined by Student's *t*-test analysis. Differences among more than 2 groups were analyzed by 2-way ANOVA and Tukey's HSD *post hoc* test. Nonnormally distributed data were normalized by log transformation for analysis. Groups were considered significantly different when the *P* value was ≤ 0.05. All statistics were performed using JMP IN software, release 5.1.2 (Copyright 1989–2004, SAS Institute Inc.).

## Results

### Localization of SHMT1 in colonic epithelial cells

SHMT1 exhibits tissue-specific expression and is present in all tissues associated with folate-mediated pathologies including the colon (19, 27, 28). Here, we show that SHMT1 is specifically expressed in the cytoplasm of mature colonic enterocytes (Fig. 2A), in mitotically active epithelial cells in the proliferative zone of colonic crypts (Fig. 2A and C), and in the nucleus of cells residing at the base of colonic crypts (Fig. 2A and E).



**Figure 2.** SHMT1 localization in mouse colonocytes. SHMT1 was detected in histologic sections of colon from wild-type FVB/NJ mice probed with polyclonal sheep anti-SHMT1 antibody. A, SHMT1 is expressed in the cytoplasm of colonic enterocytes (black arrowheads), in mitotically active epithelial cells in the proliferative zone of the colonic crypts (black arrows), and in the nucleus of cells residing in the base of the crypts (white arrows). C, magnification of mitotically active cells expressing SHMT1. E, SHMT1 is expressed in the nucleus of cells residing at the base of the colonic crypts, indicated by white arrows. B, D, and F, mouse colon probed with nonimmune sheep serum.
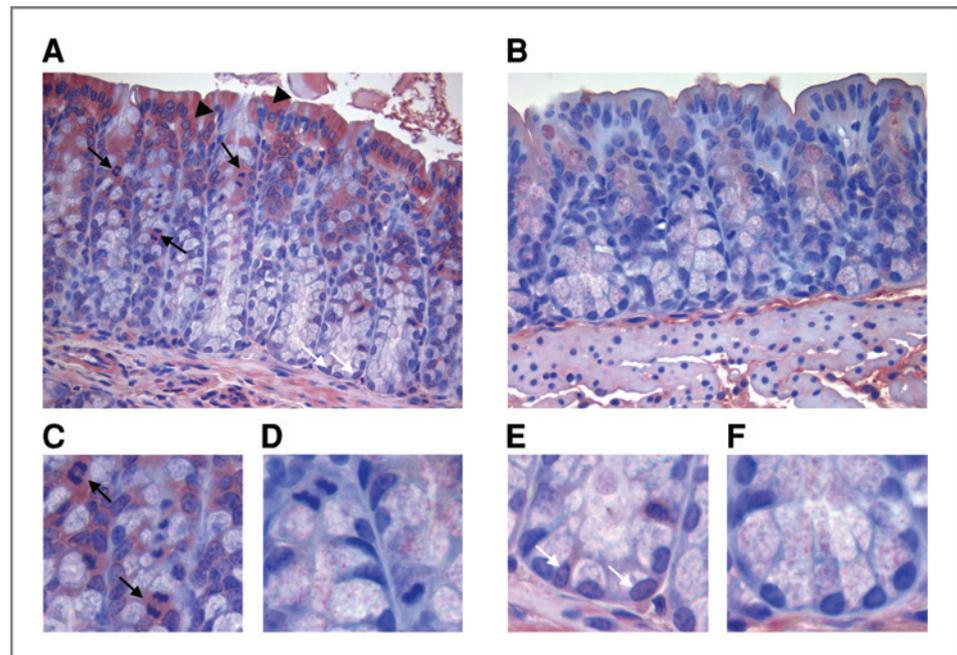
**Table 1.** Tissue folate concentrations in $Apc^{+/+}Shmt1^{-/+}$ mice on diet for 5 weeks and $Apc^{min/+}Shmt1^{-/+}$ mice on diet for 11 weeks

| Diet | *Shmt1* Genotype | $Apc^{+/+}$ mice on diet for 5 weeks | | | $Apc^{min/+}$ mice on diet for 11 weeks | |
|---|---|---|---|---|---|---|
| | | Plasma, ng/mL | Liver, fmol/µg protein | Colon, fmol/µg protein | Plasma, ng/mL | Liver, fmol/µg protein |
| Control | $Shmt1^{+/+}$ | 58.56 ± 10.75 | 51.80 ± 2.94 | 35.14 ± 10.32 | 24.68 ± 7.50 | 45.72 ± 9.50 |
| | $Shmt1^{-/+}$ | 58.34 ± 7.05 | 56.65 ± 8.39 | 21.46 ± 4.02 | 20.91 ± 5.01 | 40.00 ± 3.24 |
| | $Shmt1^{-/-}$ | 40.82 ± 7.78 | 50.77 ± 8.80 | 17.09 ± 2.10 | 26.44 ± 3.08 | 41.50 ± 2.69 |
| FCD | $Shmt1^{+/+}$ | 20.60 ± 1.80 | 47.26 ± 5.77 | 9.15 ± 2.02 | 11.79 ± 2.93 | 28.49 ± 2.68 |
| | $Shmt1^{-/+}$ | 38.95 ± 2.84 | 44.30 ± 5.59 | 18.04 ± 2.25 | 8.37 ± 1.56 | 23.25 ± 1.85 |
| | $Shmt1^{-/-}$ | 8.52 ± 8.52 | 48.88 ± 3.06 | 14.89 ± 4.24 | 9.97 ± 2.32 | 29.44 ± 2.71 |
| | P value, diet effect | 0.0003 | NS | 0.03 | 0.0009 | 0.002 |
| | P value, genotype effect | 0.02[a] | NS | NS | NS | NS |
| | P value, diet × genotype effect | NS | NS | NS | NS | NS |

NOTE: Data are presented as mean ± SEM; $n = 3–4$.
[a]$Shmt1^{-/+}$ versus $Shmt1^{-/-}$ are significantly different independent of diet; $P < 0.05$.

## SHMT1 and diet interact to influence intestinal tumor development

To determine the effect of *Shmt1* on intestinal tumor development, $Shmt1^{-/+}$ mice (19), were mated to $Apc^{min/+}$ mice, a model of spontaneous intestinal neoplasia (29). Double heterozygous offspring were intercrossed to achieve $Apc^{min/+}Shmt1^{+/+}$, $Apc^{min/+}Shmt1^{-/+}$, or $Apc^{min/+}Shmt1^{-/-}$ mice. Mice were weaned at 21 days and randomly assigned to either a control (C) or an FCD diet. Plasma and colon folate concentrations were determined in $Apc^{+/+}$ littermates after 5 weeks on diet to estimate folate status at the midpoint of the experiment. Folate in colon was significantly reduced by the FCD diet after 5 weeks (Table 1). This confirms that the colon is sensitive to dietary folate depletion (30). Liver folate concentrations were significantly reduced in mice only after 11 weeks on diet (Table 1).

The small and large intestines from $Apc^{min/+}$ mice were examined for neoplasia at 14 weeks of age, after 11 weeks on diet. In mice fed the control diet, decreased SHMT1 expression had no effect on tumor number or load (Fig. 3A and B). The
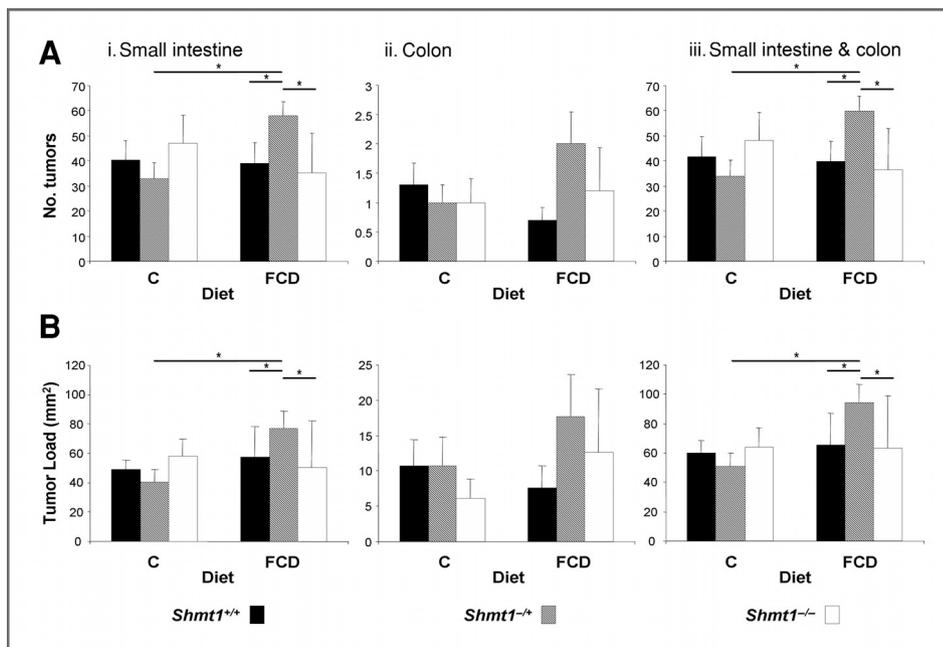


Figure 3. Tumor number and load in $Apc^{min/+}Shmt1^{+/+}$, $Apc^{min/+}Shmt1^{-/+}$ or $Apc^{min/+}Shmt1^{-/-}$ mice. A, tumor number in the small intestine (i), colon (ii), and combined small intestine and colon (iii). B, tumor load in the small intestine (i), colon (ii), and combined small intestine and colon (iii). Tumor load was calculated as the total tumor area per mouse; $n = 10–13$ for $Shmt1^{+/+}$ and $Shmt1^{-/+}$ mice, $n = 4–5$ for $Shmt1^{-/-}$ mice. Data are presented as mean ± SEM. *, $P \leq 0.05$.

FCD diet was not associated with increased tumor number or load in $Apc^{min/+}Shmt1^{+/+}$, or $Shmt1^{-/-}$ mice. However, the FCD diet was associated with more than a 50% increase in total tumor number and load in $Apc^{min/+}Shmt1^{-/+}$ mice (Fig. 3A and B). The effect in $Apc^{min/+}Shmt1^{-/+}$ mice on tumor number was driven by an approximately 50% increase in small intestinal tumors and a doubling of colon tumors, although the latter was not statistically significant

### *De novo* purine synthesis is not dependent on SHMT1 status

To determine the mechanism by which *Shmt1* hemizygosity modifies CRC susceptibility in $Apc^{min/+}$ mice, the effects of SHMT1 depletion on *de novo* purine and thymidylate biosynthesis and cellular methylation potential were determined. MEFs were used to determine the impact of *Shmt1* hemizygosity on *de novo* nucleotide synthesis relative to synthesis by the salvage pathway. We found that *de novo* purine synthesis relative to synthesis by the salvage pathway was not significantly affected by *Shmt1* genotype in MEFs (Fig. 4A).

### SHMT1, cellular methylation potential, and gene expression

Our previous data suggest that $Shmt1^{-/-}$ mice have increased hepatic AdoMet concentrations compared with wild-type and hemizygous mice under conditions of folate depletion (19). However, AdoMet and AdoHcy levels, as well as the AdoMet/AdoHcy ratio, were not significantly affected by *Shmt1* genotype or diet in this study (Table 2).

In addition, we performed a microarray analysis on colons from mice fed the FCD diet to determine the effect of *Shmt1* on gene expression and its relationship to tumor susceptibility. Using the NuGen Ovation amplification approach, a Present Call of between 78% and 81% was achieved, indicating high sensitivity in transcript detection. However, at a *P* value of 0.01, less than 10 genes in *Shmt1* hemizygous mice and less than 15 genes in null mice of the possible 19,000 present genes had a 2-fold or greater change in gene expression. These minimal differences strongly suggest that gene expression changes in *Shmt1* mutants would be difficult to detect (Supplementary Table S1). The data were confirmed by qRT-PCR for 9 genes of interest (Supplementary Table S2). Only one gene, uridine phosphorylase (*Upp1*), demonstrated consistent changes in expression.

### SHMT1 modifies thymidylate synthesis capacity

Previously, we have shown that uracil content in hepatic nuclear DNA was significantly affected by *Shmt1* genotype (19). Here, we have found that uracil content in hepatic nuclear DNA, which correlates with colon uracil content in *Shmt1* knockout mice (A.J. MacFarlane and P.J. Stover, in preparation), was significantly increased in $Apc^{min/+}Shmt1^{-/+}$ mice in comparison with $Apc^{min/+}Shmt1^{+/+}$ mice, and uracil content doubled when the $Apc^{min/+}Shmt1^{-/+}$ mice were fed the FCD diet (Table 2). Although uracil content also doubled in $Apc^{min/+}Shmt1^{+/+}$ fed the FCD diet, the absolute concentration was consistently one third of that observed in
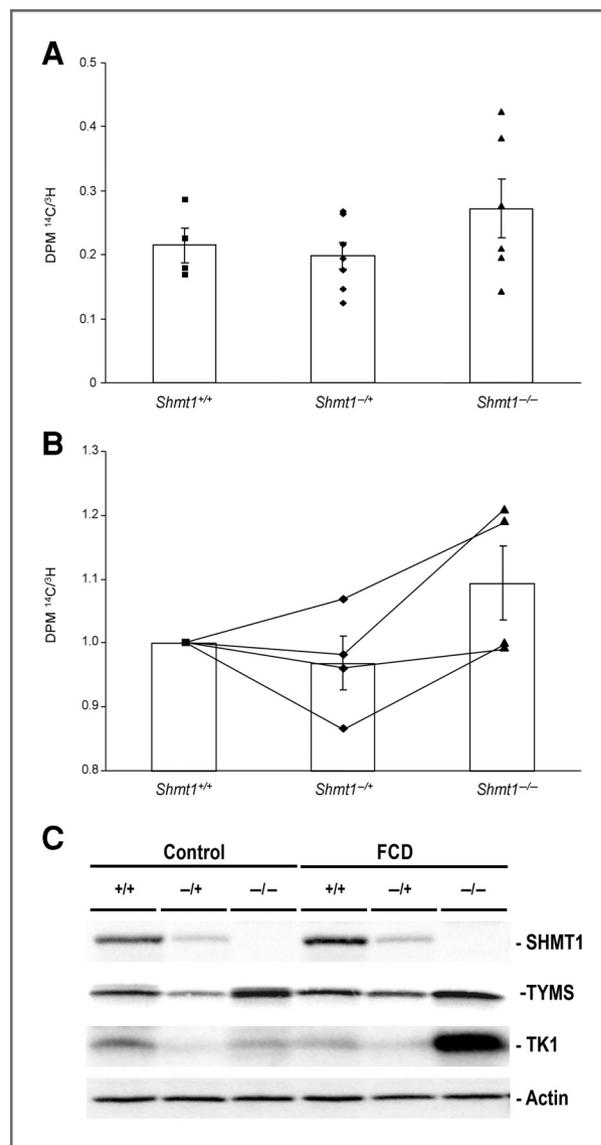


**Figure 4.** Purine and thymidylate synthesis. A, [$^{14}$C]formate and [$^{3}$H]hypoxanthine are precursors for purine nucleotide biosynthesis through the *de novo* and salvage pathways, respectively. Data are presented as a ratio of *de novo* to salvage purine synthesis, [$^{14}$C]formate/ [$^{3}$H]hypoxanthine; *n* = 4–7 independent MEF lines per genotype. B, [$^{14}$C]Deoxyuridine and [$^{3}$H]thymidine are precursors for thymidylate nucleotide biosynthesis through the *de novo* and salvage pathways, respectively. Data are presented as a ratio of *de novo* to salvage thymidylate synthesis, [$^{14}$C]deoxyuridine/[$^{3}$H]thymidine. *P* = 0.08 for a genotype effect; *n* = 4 independent MEF lines per genotype. Data were normalized to wild-type for independent experiments. Lines connect independent experiments. C, representative Western blots for SHMT1, TYMS, TK1, and actin in colon tissue from $Apc^{+/+}Shmt1^{+/+}$, $Shmt1^{-/+}$, and $Shmt1^{-/-}$ mice fed either a control or FCD diet for 5 weeks from weaning.

$Apc^{min/+}Shmt1^{-/+}$ regardless of diet. In addition, MEFs derived from $Shmt1^{-/+}$ mice demonstrated a tendency for decreased *de novo* thymidylate synthesis relative to the salvage pathway in comparison with $Shmt1^{+/+}$ MEFs as determined by a modified deoxyuridine suppression assay (ref. 31; Fig. 4B).

**Table 2.** Liver AdoMet, AdoHcy, AdoMet/AdoHcy ratio, and uracil content in nuclear DNA in $Apc^{min/+}$ $Shmt1^{-/+}$ mice after 11 weeks on diet

| Diet | Shmt1 Genotype | AdoMet, pmol/µg protein | AdoHcyc, pmol/µg protein | AdoMet/AdoHcy | Uracil, pg/µg DNA |
|---|---|---|---|---|---|
| AIN-93G | $Shmt1^{+/+}$ | 1.4 ± 0.4 | 0.9 ± 0.2 | 1.9 ± 0.4 | 0.1 ± 0.1 |
| | $Shmt1^{-/+}$ | 0.8 ± 0.2 | 0.6 ± 0.0 | 1.5 ± 0.3 | 0.3 ± 0.1 |
| | $Shmt1^{-/-}$ | 1.5 ± 0.3 | 0.9 ± 0.1 | 1.7 ± 0.4 | 0.1 ± 0.0 |
| AIN-93G minus folate and choline | $Shmt1^{+/+}$ | 1.4 ± 0.4 | 0.7 ± 0.1 | 1.9 ± 0.4 | 0.2 ± 0.0 |
| | $Shmt1^{-/+}$ | 0.8 ± 0.1 | 0.6 ± 0.1 | 1.3 ± 0.1 | 0.6 ± 0.2 |
| | $Shmt1^{-/-}$ | 1.9 ± 0.8 | 0.8 ± 0.2 | 2.0 ± 0.6 | 0.2 ± 0.1 |
| | P value, diet effect | NS | NS | NS | 0.06 |
| | P value, genotype effect | 0.10 | NS | NS | 0.01[a] |
| | P value, diet × genotype effect | NS | NS | NS | NS |

NOTE: Data are presented as mean ± SEM values; $n$ = 3–7 per group.
[a]$Shmt1^{-/+}$ versus $Shmt1^{+/+}$ and $Shmt1^{-/-}$ are significantly different independent of diet; $P < 0.05$.

Furthermore, the protein expression of TYMS, which functions in *de novo* thymidylate synthesis, was decreased in the colon of $Shmt1^{-/+}$ mice in comparison with wild-type mice fed the control diet (Fig. 4C; 0.69 ± 0.3 vs. 1.00 ± 0.04). TK1 protein expression was not different between hemizygous and wild-type mice. The data indicate that $Shmt1^{-/+}$ mice experience a reduction in *de novo* thymidylate synthesis capacity relative to their wild-type counterparts, which likely accounts for the increased incorporation of uracil into nuclear DNA observed in these mice.

Surprisingly, $Shmt1^{-/-}$ mice had lower uracil levels in nuclear DNA compared with $Shmt1^{-/+}$ mice (Table 2) and MEFs from $Shmt1^{-/-}$ mice exhibited increased *de novo* thymidylate biosynthesis relative to synthesis from salvage compared with those derived from $Shmt1^{-/+}$ mice (Fig. 4B). $Shmt1^{-/-}$ mice demonstrated markedly elevated colonic TYMS (2.86 ± 1.3 vs. 1.00 ± 0.04) and TK1 (2.19 ± 1.0 vs. 0.97 ± 0.06) protein expression in comparison to $Shmt1$ wild-type mice. Although the results were unexpected, the changes in TYMS and TK1 protein expression observed in $Shmt1^{-/-}$ mice could explain their increased capacity for thymidylate synthesis and decreased uracil concentration in genomic DNA in comparison with $Shmt1^{-/+}$ mice.

### Dietary folate regulation of SHMT1, TYMS, and TK1

In addition to $Shmt1$-dependent changes to thymidylate synthesis capacity, we also observed an upregulation of members of the *de novo* and salvage dTMP biosynthetic pathways in response to folate deficiency. SHMT1 protein was increased by 35% (1.2 ± 0.4 vs. 0.9 ± 0.1), and TYMS protein was increased by 80% (1.8 ± 0.6 vs. 1.00 ± 0.04), as determined by densitometry, in the colons of $Shmt1$ wild-type mice fed the FCD diet in comparison to control fed mice (Fig. 4C), which could account for the lack of an effect of folate deficiency on uracil content in DNA (Table 2) and intestinal tumor number and load in wild-type mice (Fig. 3A and B).

Although SHMT1 (0.56 ± 0.2 vs. 0.4 ± 0.06) and TYMS (1.7 ± 0.5 vs. 0.7 ± 0.3) levels were also increased in $Shmt1^{-/+}$ mice fed the FCD diet, the absolute levels of these enzymes never exceeded than those observed in wild-type mice (Fig. 4C). TK1 protein levels were also increased when wild-type mice were fed the FCD diet (1.0 ± 0.06 vs. 2.0 ± 0.8), which could support an increased capacity to synthesize thymidylate from the salvage pathway and also contribute to their protection from diet-mediated cancer susceptibility. TK1 also increased in $Shmt1^{-/+}$ mice fed the FCD diet (1.5 ± 0.1 vs. 1.0 ± 0.6), but the induction was to a lesser extent than that observed in wild-type mice. Finally, TK1 remained high but unchanged in $Shmt1^{-/-}$ mice fed the FCD diet (2.0 ± 0.5 vs. 2.2 ± 1.1).

## Discussion

Altered folate metabolism has been shown to be a risk factor for the development of CRC. However, the mechanism (s) involved remain unknown. Because of its metabolic properties and its cellular localization, SHMT1 is poised to regulate 1C metabolism in cells associated with neoplastic transformation and CRC risk (32). Therefore, SHMT1 expression was modified to determine the relative contributions of dTMP, purine, and AdoMet synthesis and consequently indicators of genome stability and methylation, to intestinal tumorigenesis.

Three biosynthetic pathways, purine, thymidylate, and methionine synthesis, compete for 5,10-methyleneTHF, a limited cofactor in the cell. C1THF synthase can convert 5,10-methyleneTHF to 10-formylTHF, the substrate required for *de novo* synthesis of purines (33). Whereas purine deprivation or inhibition of *de novo* purine synthesis is usually associated with $G_1$ arrest, cytostasis, and cytotoxicity (34, 35), reduced purine synthesis capacity has also been associated with abnormal DNA repair and DNA mutagenesis in

mammalian cells (36, 37) and could thereby play a role in *Apc*-mediated intestinal tumorigenesis. However, we observed that *de novo* purine synthesis relative to synthesis by the salvage pathway was not significantly affected by *Shmt1* genotype in MEFs and therefore does not likely contribute to the increased tumor numbers observed in *Apc^{min/+}Shmt1^{-/+}* mice.

5,10-MethyleneTHF can also be irreversibly reduced by methyleneTHF reductase (MTHFR) to form 5-methyTHF, from which a methyl group is transferred to homocysteine by methionine synthase (MS) to form methionine. Methionine can then be *S*-adenosylated to form AdoMet, the major methyl donor in cellular methylation reactions. The balance between AdoMet and AdoHcy, the substrate and product, respectively, of transmethylation reactions is an indicator of cellular methylation potential. Cellular methylation potential can impact DNA, RNA, and histone methylation patterns and has been associated with aberrant gene expression patterns in cancer. SHMT1 regulates the partitioning of methyl groups between the thymidylate and methionine synthesis pathways by preferentially shuttling its product, 5,10-methyleneTHF, toward thymidylate synthesis, as well as by tightly binding 5-methylTHF making it unavailable to the methionine cycle (14). *Apc^{min/+}Shmt1^{-/-}* mice tended to have increased hepatic AdoMet under folate-deficient conditions; however, unlike our previous findings, the difference was not statistically significant (19). We determined *Shmt1*-dependent changes in gene expression patterns in hemizygous mice fed the FCD diet, which were minimal, with only 10 genes identified that had significant changes in expression greater than 2-fold in *Shmt1^{-/+}* mice compared with wild-type mice. One interesting note is that the only gene that demonstrated consistent changes in expression, as confirmed by RT-PCR, was *Upp1*, which is involved in pyrimidine degradation and uridine homeostasis, indicating another mechanism by which SHMT1 status could impact thymidylate synthesis capacity (38). A limitation to our microarray analysis was that it did not determine diet or gene-by-diet effects as mice fed the control diet were not included in the analysis. However, together the data suggest that cellular methylation potential and any associated changes in gene expression did not significantly contribute to tumorigenesis in this mouse model.

Finally, 5,10-methyleneTHF can be utilized by TYMS to methylate dUMP for the *de novo* synthesis of dTMP. We have shown that SHMT1 preferentially partitions 1C units into the *de novo* thymidylate biosynthetic pathway (14). Consistent with our previous observations, we saw a decrease in *de novo* thymidylate synthesis in *Shmt1^{-/+}* mice, which was associated with an increase in uracil incorporation into nuclear DNA. Interestingly, *Shmt1^{-/+}* mice also demonstrated decreased TYMS protein expression. TK1 was induced by the FCD diet in hemizygous mice, but to a lesser extent than that observed in wild-type mice. A reduction in TK1 would result in decreased uptake of thymidine from the salvage pathway, in addition to an overall dampening of the capacity to synthesize dUMP, and subsequently dTMP, whereas a reduction in TYMS would specifically decrease the capacity for *de*

*novo* thymidylate synthesis. We conclude that impairments in *de novo* thymidylate biosynthesis, resulting from *Shmt1* hemizygosity and its consequent effect on TYMS and TK1 protein levels, exacerbate the tumor phenotype of *Apc^{min/+}* mice fed the FCD diet. Observed increases in SHMT1, TYMS, and TK1 in wild-type mice fed the FCD diet or dramatic increases in TYMS and TK1 in *Shmt1^{-/-}* mice could serve as a protective mechanism to maintain adequate dTMP synthesis thereby minimizing uracil misincorporation into nuclear DNA and consequent genome instability.

In the *Apc^{min/+}* mouse model of CRC, *Shmt1* hemizygosity did not significantly affect either *de novo* purine synthesis or cellular methylation potential, indicating that these pathways were unlikely to contribute to the increased tumorigenesis observed in *Shmt1^{-/+}* mice. However, changes in dTMP synthesis were significantly and inversely correlated with increased risk for intestinal cancer development in a gene-by-diet interaction. Furthermore, *de novo* thymidylate synthesis capacity appears to be dynamically regulated by diet and *Shmt1* expression. TYMS and TK1 protein levels respond to changes in SHMT1 expression, and TYMS, TK1, and SHMT1 levels respond to dietary folate/choline deficiency. As a result of these dynamic changes, thymidylate synthesis capacity, as indicated by uracil content in nuclear DNA and metabolic flux assays in MEFs, was lowest in *Shmt1^{-/+}* mice, which exhibited the highest tumor number and load in *Apc^{min/+}* mice under FCD conditions.

Loss of heterozygosity of the *Apc* gene is an early and necessary event for intestinal neoplastic transformation in the *Apc^{min/+}* mice (39). It has previously been shown that colonic folate concentrations correlate with strand breaks in the *Apc* gene in rats fed a severely folate deficient diet for 5 weeks and that the strand breaks were inversely correlated with steady-state transcript levels of *Apc* (18). In addition, mild folate depletion in combination with other B vitamins, including vitamins B6 and B12, and methionine, was associated with DNA strand breaks within the *Apc* mutation cluster region, decreased expression of a number of genes involved in the Wnt signaling pathway, and suppression of apoptosis in colonocytes (30). The increased uracil misincorporation into DNA and subsequent genome instability associated with *Shmt1* hemizygosity in combination with dietary folate deficiency accelerated the loss of heterozygosity of the *Apc* gene and resulted in increased cellular transformation and tumor development. Compensatory mechanisms appear to buffer thymidylate synthesis capacity under folate-restricted conditions, as demonstrated by the upregulation of SHMT1, TYMS, and TK1 in the colon of FCD-fed mice, which provide protection from loss of *Apc* heterozygosity and tumorigenesis. Together, our data provide a plausible mechanism by which folate-dependent thymidylate synthesis and consequential changes to genomic stability contribute to *Apc*-mediated intestinal cancer.

## Disclosure of Potential Conflicts of Interest

No potential conflicts of interest were disclosed.

## References

1. Giovannucci E, Stampfer MJ, Colditz GA, Rimm EB, Trichopoulos D, Rosner BA, et al. Folate, methionine, and alcohol intake and risk of colorectal adenoma. J Natl Cancer Inst 1993;85:875–84.
2. Ma J, Stampfer MJ, Giovannucci E, Artigas C, Hunter DJ, Fuchs C, et al. Methylenetetrahydrofolate reductase polymorphism, dietary interactions, and risk of colorectal cancer. Cancer Res 1997;57:1098–102.
3. Kim J, Kim DH, Lee BH, Kang SH, Lee HJ, Lim SY, et al. Folate intake and the risk of colorectal cancer in a Korean population. Eur J Clin Nutr 2009;63:1057–64.
4. Cole BF, Baron JA, Sandler RS, Haile RW, Ahnen DJ, Bresalier RS, et al. Folic acid for the prevention of colorectal adenomas: a randomized clinical trial. JAMA 2007;297:2351–9.
5. Logan RF, Grainge MJ, Shepherd VC, Armitage NC, Muir KR. Aspirin and folic acid for the prevention of recurrent colorectal adenomas. Gastroenterology 2008;134:29–38.
6. Shane B. Folate chemistry and metabolism. In: Bailey LB, editor. Folate in health and disease. New York: Marcel Dekker Inc.; 1995. p. 1–22.
7. Fox JT, Stover PJ. Folate-mediated one-carbon metabolism. Vitam Horm 2008;79:1–44.
8. James SJ, Yin L. Diet-induced DNA damage and altered nucleotide metabolism in lymphocytes from methyl-donor-deficient rats. Carcinogenesis 1989;10:1209–14.
9. Branda RF, Blickensderfer DB. Folate deficiency increases genetic damage caused by alkylating agents and gamma-irradiation in Chinese hamster ovary cells. Cancer Res 1993;53:5401–8.
10. Duthie SJ, Hawdon A. DNA instability (strand breakage, uracil misincorporation, and defective repair) is increased by folic acid depletion in human lymphocytes *in vitro*. FASEB J 1998;12:1491–7.
11. Wainfan E, Poirier LA. Methyl groups in carcinogenesis: effects on DNA methylation and gene expression. Cancer Res 1992;52:2071S–7.
12. Friso S, Choi SW, Girelli D, Mason JB, Dolnikowski GG, Bagley PJ, et al. A common mutation in the 5,10-methylenetetrahydrofolate reductase gene affects genomic DNA methylation through an interaction with folate status. Proc Natl Acad Sci U S A 2002;99:5606–11.
13. Gaudet F, Hodgson JG, Eden A, Jackson-Grusby L, Dausman J, Gray JW, et al. Induction of tumors in mice by genomic hypomethylation. Science 2003;300:489–92.
14. Herbig K, Chiang EP, Lee LR, Hills J, Shane B, Stover PJ. Cytoplasmic serine hydroxymethyltransferase mediates competition between folate-dependent deoxyribonucleotide and S-adenosylmethionine biosyntheses. J Biol Chem 2002;277:38381–9.
15. Anderson DD, Stover PJ. SHMT1 and SHMT2 are functionally redundant in nuclear *de novo* thymidylate biosynthesis. PLoS ONE 2009;4:e5839.
16. Woeller CF, Anderson DD, Szebenyi DM, Stover PJ. Evidence for small ubiquitin-like modifier-dependent nuclear import of the thymidylate biosynthesis pathway. J Biol Chem 2007;282:17623–31.
17. Fodde R, Brabletz T. Wnt/beta-catenin signaling in cancer stemness and malignant behavior. Curr Opin Cell Biol 2007;19:150–8.
18. Kim YI, Shirwadkar S, Choi SW, Puchyr M, Wang Y, Mason JB. Effects of dietary folate on DNA strand breaks within mutation-prone exons of the p53 gene in rat colon. Gastroenterology 2000;119:151–61.
19. MacFarlane AJ, Liu X, Perry CA, Flodby P, Allen RH, Stabler SP, et al. Cytoplasmic serine hydroxymethyltransferase regulates the metabolic partitioning of methylenetetrahydrofolate but is not essential in mice. J Biol Chem 2008;283:25846–53.
20. Liu X, Szebenyi DM, Anguera MC, Thiel DJ, Stover PJ. Lack of catalytic activity of a murine mRNA cytoplasmic serine hydroxymethyltransferase splice variant: evidence against alternative splicing as a regulatory mechanism. Biochemistry 2001;40:4932–9.
21. Chiu CH, McEntee MF, Whelan J. Sulindac causes rapid regression of preexisting tumors in Min/ +mice independent of prostaglandin biosynthesis. Cancer Res 1997;57:4267–73.
22. Bensadoun A, Weinstein D. Assay of proteins in the presence of interfering materials. Anal Biochem 1976;70:241–50.
23. Field MS, Szebenyi DM, Stover PJ. Regulation of *de novo* purine biosynthesis by methenyltetrahydrofolate synthetase in neuroblastoma. J Biol Chem 2006;281:4215–21.
24. The R Project for Statistical Computing [cited 2010 March 1]. Available from:http://www.r-project.org/.
25. Edgar R, Domrachev M, Lash AE. Gene Expression Omnibus: NCBI gene expression and hybridization array data repository. Nucleic Acids Res 2002;30:207–10.
26. Universal ProbeLibrary [cited 2010 March 1]. Available from: https://www.roche-applied-science.com/sis/rtpcr/upl/index.htm
27. Girgis S, Nasrallah IM, Suh JR, Oppenheim E, Zanetti KA, Mastri MG, et al. Molecular cloning, characterization and alternative splicing of the human cytoplasmic serine hydroxymethyltransferase gene. Gene 1998;210:315–24.
28. Stover PJ, Chen LH, Suh JR, Stover DM, Keyomarsi K, Shane B. Molecular cloning, characterization, and regulation of the human mitochondrial serine hydroxymethyltransferase gene. J Biol Chem 1997;272:1842–8.
29. Su LK, Kinzler KW, Vogelstein B, Preisinger AC, Moser AR Luongo C, et al. Multiple intestinal neoplasia caused by a mutation in the murine homolog of the APC gene. Science 1992;256:668–70.
30. Liu Z, Choi SW, Crott JW, Keyes MK, Jang H, Smith DE, et al. Mild depletion of dietary folate combined with other B vitamins alters multiple components of the Wnt pathway in mouse colon. J Nutr 2007;137:2701–8.
31. Killmann SA. Effect of deoxyuridine on incorporation of tritiated thymidine: difference between normoblasts and megaloblasts. Acta Med Scand 1964;175:483–8.
32. Radtke F, Clevers H. Self-renewal and cancer of the gut: two sides of a coin. Science 2005;307:1904–9.
33. Tan LU, Drury EJ, MacKenzie RE. Methylenetetrahydrofolate dehydrogenase-methenyltetrahydrofolate cyclohydrolase-formyltetrahydrofolate synthetase. A multifunctional protein from porcine liver. J Biol Chem 1977;252:1117–22.
34. Kondo M, Yamaoka T, Honda S, Miwa Y, Katashima R, Moritani M, et al. The rate of cell growth is regulated by purine biosynthesis via

ATP production and G(1) to S phase transition. J Biochem 2000;128:57–64.

35. Bronder JL, Moran RG. Antifolates targeting purine synthesis allow entry of tumor cells into S phase regardless of p53 function. Cancer Res 2002;62:5236–41.

36. Mathews CK. DNA precursor metabolism and genomic stability. FASEB J 2006;20:1300–14.

37. Collins AR, Black DT, Waldren CA. Aberrant DNA repair and enhanced mutagenesis following mutagen treatment of Chinese hamster Ade-C cells in a state of purine deprivation. Mutat Res 1988;193:145–55.

38. Pizzorno G, Cao D, Leffert JJ, Russell RL, Zhang D, Handschumacher RE. Homeostatic control of uridine and the role of uridine phosphorylase: a biological and clinical update. Biochim Biophys Acta 2002;1587:133–44.

39. Levy DB, Smith KJ, Beazer-Barclay Y, Hamilton SR, Vogelstein B, Kinzler KW. Inactivation of both APC alleles in human and mouse tumors. Cancer Res 1994;54:5953–8.